

Published in final edited form as:

Curr Top Med Chem. 2010 ; 10(12): 1147–1157.

Near-Infrared Quantum Dots as Optical Probes for Tumor Imaging

Jinhao Gao^{*,1}, Xiaoyuan Chen², and Zhen Cheng¹

¹Molecular Imaging Program at Stanford, Department of Radiology and Bio-X Program, School of Medicine, Stanford University, 1201 Welch Road, Stanford, CA 94305-5484, USA

²National Institute of Biomedical Imaging and Bioengineering, National Institutes of Health, 31 Center Drive, Bethesda, MD 20892-2281, USA

Abstract

Molecular imaging plays a key role in personalized medicine, which is the goal and future of patient management. Among the various molecular imaging modalities, optical imaging may be the fastest growing area for bioanalysis, and the major reason is the research on fluorescence semiconductor quantum dots (QDs) and dyes have evolved over the past two decades. The great efforts on the synthesis of QDs with fluorescence emission from UV to near-infrared (NIR) regions speed up the studies of QDs as optical probes for *in vitro* and *in vivo* molecular imaging. For *in vivo* applications, the fluorescent emission wavelength ideally should be in a region of the spectrum where blood and tissue absorb minimally and tissue penetration reach maximally, which is NIR region (typically 700–1000 nm). The goal of this review is to provide readers the basics of NIR-emitting QDs, the bioconjugate chemistry of QDs, and their applications for diagnostic tumor imaging. We will also discuss the benefits, challenges, limitations, perspective, and the future scope of NIR-emitting QDs for tumor imaging applications.

Keywords

Quantum dots; near-infrared; tumor imaging; fluorescence imaging; perspective

1. INTRODUCTION

This review describes the application of quantum dots (QDs) with near-infrared (NIR) emission for *in vivo* tumor imaging. Over the past decades, the research of nanotechnology has grown explosively covering the fields of materials, energy, electronics, biology, and medicine. The integration of nanotechnology with molecular biology and medicine has resulted in active developments of a new emerging research area—nanobiotechnology [1, 2]. Nanobiotechnology is defined as a field that applies the nanoscale principles, materials, and techniques to understand and transform biosystems, and which uses biological principles and materials to create new devices and systems integrated from the nanoscale [1]. This technological innovation, referred to nanomedicine by the National Institutes of Health (NIH), has great potential to offer exciting and abundant opportunities for discovering new materials and tools in biomedicine. One of the most advanced and exciting forefronts of nanobiotechnology is the various applications of QDs in biology and medicine [3]. Compared with the organic dyes and fluorescent proteins, QDs show many unique optical

properties, such as symmetrical, narrow, and tunable emission spectra, superior photostability, high quantum yields, and the capacity of simultaneous excitation of multiple fluorescence colors. Moreover, there are much more alternatives in QDs with NIR emission for *in vivo* imaging than organic dyes [4]. The QDs emitting at above 700 nm in the NIR region minimize the problems of endogenous fluorescence of tissues and meet the requirements of *in vivo* biological imaging applications.

Cancer is a serious burden for the public health in the world because cancer cells are very aggressive and invasive. In 2007, the NIH estimated an overall cost of \$206.3 billion as a result of cancer. There are many traditional medical imaging techniques to detect cancer and monitor the therapeutic effects of cancer intervention, such as computed tomography (CT), magnetic resonance imaging (MRI), and ultrasound. The field of molecular imaging, recently defined by the Society of Nuclear Medicine (SNM) as “the visualization, characterization, and measurement of biological processes at the molecular and cellular levels in humans and other living systems” [5], has flourished over the last decades. Among the various molecular imaging modalities, optical imaging may be the fastest growing area for *in vivo* analysis, [6, 7] mainly because the research on biomedical applications of QDs and other fluorescent materials has evolved over the past two decades. The development of high-sensitivity and high-specificity molecular probes is of considerable interest in many areas of cancer research, ranging from basic tumor biology to *in vivo* imaging and early detection. Non-invasive fluorescent imaging of preclinical animal models *in vivo* is a rapidly developing field with new emerging techniques. QD fluorescent probes with longer emission wavelengths in NIR emission ranges are more amenable to deep-tissue imaging, because both scattering and autofluorescence are reduced as wavelengths are increased [8]. After the surface functionalization using peptides, proteins, and antibodies, QDs have indeed shown great ability to target and detect specific tissues in living subjects by the rapid readout of fluorescence imaging [9–16]. In this review article, we focus on the NIR-fluorescence emitting QDs, from synthesis to modification, from bioconjugation to targeted imaging, from fluorescence imaging to multimodality imaging, and from critical comments to perspective. We hope to arouse readers more interests and attentions on the future scope of NIR-emitting QDs for fluorescence imaging applications.

2. NEAR-INFRARED QUANTUM DOTS

In order to meet the requirements of *in vivo* biological imaging applications, the fluorescent emission wavelengths of the QDs ideally should be in a region of the spectrum where blood and tissue absorb minimally but still detectable by the instruments. Thus, the QDs should emit at approximately 700–1000 nm in the NIR region to minimize the problems of endogenous fluorescence of tissues. As shown in Fig (1), the emission wavelength of the colloidal QDs made of ZnS, CdSe, CdTe, PbS, PbSe, and InAs has covered from the UV to the infrared range. Because of their wide absorption spectra, QDs with different emission wavelengths excited by a single light source can emit various color fluorescence, therefore, QDs have a great potential for multicolor molecular imaging. Considering the toxicity and instability of CdTe and InAs QDs surface, it is extremely important to passivate or cap the CdTe and InAs QDs with a layer of ZnS or ZnSe. This layer protects the QDs against photo-oxidation as well as improves the fluorescence quantum yield of the QDs. The ZnS shell has larger bandgap energy than CdTe, eliminating the core's surface defect states. The strategy of using ZnS or ZnSe shell to cap QDs has become a popular approach. Because of high interest and demand of NIR QDs, the development on the synthesis of NIR QDs based on this approach has progressed rapidly, such as CdTe/ZnS [17], CdTe/CdSe [18], InAs_xP_{1-x}/InP/ZnSe [19], CuInSe [20], and Cu-doped InP/ZnSe [21] QDs. However, it is reported that the Cd-containing QDs indeed shows cytotoxicity under extreme conditions [22, 23]. For *in vivo* applications, metabolic clearance of the nanoparticles remains an issue, that is, it is

hard to know about how these nanoparticles would be completely cleared out of the body. To avoid such a dilemma, one strategy is to replace the Cd metal by other more benign elements. For example, CuInS₂/ZnS core/shell QDs do not contain any Class A elements (Cd, Pb, and Hg) [24], which may show great potential as biocompatible materials for biomedical applications. Recently, carbon dots (C-dots) as new emerging optical probes have aroused research interests because of their non-toxicity comparing with semiconductor QDs [25].

3. SURFACE MODIFICATION AND BIOCONJUGATION

Most of QDs synthesized in high temperature organic phases are nonpolar coated with organic ligands (e.g., trioctyl phosphine oxide (TOPO) and octadecylamine (ODA)) and insoluble in aqueous solvents. In order to render the QDs water-soluble and prevent the aggregation or precipitation of QDs in aqueous solution, surface modification of the nanoparticles is necessary. As shown in Fig. (2), there are two major strategies for the preparation of the water-soluble QDs [26]. One is chemical exchange of native organic ligands on the QDs with thiolated water-soluble ligands in a water-organic two-phase system (Fig. 2A). The most common thiolated molecules used to stabilize semiconductor QDs in aqueous media are thiolated aliphatic carboxylic acids, such as mercaptoacetic acid (MAA) [27], mercaptopropionic acid (MPA) [28–30], or mercaptoundecanoic acid (MUA). The dihydrolipoic acid (DHLA) ligands provide stable interactions with the QD surfaces owing to the bidentate chelate effect of the dithiol groups [31, 32]. Also, lipoic acid units tethered to polyethylene glycol (PEG) spacers are excellent candidates to modify QDs and further conjugate QDs with biomolecules [32–34]. These modifiers eliminate nonspecific adsorption processes and also provide anchoring sites for the covalent immobilization of the biomolecules. Other thiol-containing materials, such as peptides containing cysteine unit can also replace the organic ligands and produce water-soluble QDs [35, 36]. Recently, using water-soluble dendrons to exchange ODA can stabilize QDs and yield water-soluble QDs with high quantum yields [37]. Another strategy is hydrophobic-hydrophobic interaction between native organic ligands and amphiphilic molecules, such as amphiphilic polymers and phospholipids (Fig. 2B) [38–41]. However, the mean diameter of the resulting QDs is much larger than that of the MPA or cystamine conjugated QDs. Such excessive size may hinder the widespread implementation of QDs for *in vivo* molecular imaging. Moreover, amphiphilic polymers often lead to highly increase the surface charge resulting in nonspecific binding to cell membranes. PEGylation of the polymer coated QDs could reduce the nonspecific binding and adsorption. Nonspecific binding events are minimized in the hydroxy-PEG coated QDs and the carboxy-PEG coated QDs. On the contrary, the amine-PEG coated QDs show the significant enhancement of nonspecific binding, because they exhibit the high positive charges which lead to increase the electrostatic interaction with the cell membrane [42].

After the water solubilization of QDs, the further attachments of biomolecules (e.g., avidin, peptides, proteins, and antibodies) on their surface endow QDs with the biological activity [43], as shown in Fig. (3). The most common methods involve the coupling of primary amines in the biomolecules to the carboxylic acid residues on the encapsulating layer associated with the QDs using 1-Ethyl-3-(3-dimethylaminopropyl)-carbodiimide (EDC), for example, DOTA conjugated QDs [44, 45]. Peptides, proteins, and antibodies that containing free exposed thiol groups have the potential to conjugate with QDs that have free amine functionalities in their capping layer using heterobifunctional crosslinkers, such as 4-maleimidobutyric acid N-succinimidyl ester and succinimidyl 4-(*N*-maleimidomethyl) cyclohexane-1-carboxylate (SMCC) [46–48]. Because a polyhistidine tag consisting of six histidine residues binds carboxy-functionalized QDs, the assembly of desired biomolecules

on surfaces of QDs can be achieved by adding polyhistidine tagged proteins [42], antibodies [49], short peptides [50], or DNA [51].

4. TUMOR-TARGETED NIR FLUORESCENCE IMAGING

In vivo tumor-targeted imaging with biocompatible QDs has recently become possible in mouse models. Because of the limited tissue penetration and intense scattering of light, optical imaging will be possible in humans only at limited sites, such as tissues and lesions close to the skin surface and tissues accessible by endoscopy and during intraoperative visualization [52, 53]. The NIR fluorescence imaging approach, in which the absorbance spectra for all biomolecules reach minima, thus provides a clear window for *in vivo* optical imaging [54, 55], may have better opportunities for visualizing tumor in both small-animal models and even clinical settings. So NIR QDs after functionalization show great potential as optical probes for *in vivo* molecular imaging. Herein, we will give several examples that using NIR QDs as optical probes for *in vivo* fluorescence imaging and discuss the limitations, challenges, and perspective in their future developments.

4.1. Passive Targeting

Under *in vivo* conditions, there are two modes for the tumor-targeting of entities: passive targeting and active targeting. In the passive mode, macromolecules and nanometer-sized particles accumulate preferentially at tumor sites through an enhanced permeability and retention (EPR) effect because (i) angiogenic tumors produce vascular endothelial growth factors (VEGF) that hyperpermeabilize the tumor-associated neovasculatures and cause leakage of circulating macromolecules and small nanoparticles; and (ii) tumors lack an effective lymphatic drainage system, which leads to accumulation of macromolecules or nanoparticles in tumors [56, 57]. In fact, almost all of the approved targeting systems for anticancer drugs are of passive targeting [58]. For the passive delivery of QDs, the efficiency of targeting highly relies on the inherent physicochemical properties of the QDs (e.g., particles size, charge, and surface properties). Recently, Chen *et al.* reported the high tumor-uptake of ultrasmall NIR non-cadmium QDs due to the EPR effect [29]. One critical issue for the *in vivo* applications of QDs is the hydrodynamic diameter (HD) of nanoparticles. QDs with large size (>20 nm in diameter) suffer from extremely high reticuloendothelial system (RES) uptake, which reduce their efficiency and sensitivity. The ultrasmall water-soluble QDs (<10 nm) have attracted more and more attentions because of their unique properties and the advantages for *in vivo* applications, that is, the rapid renal clearance [59, 60], low RES uptake, and high possibility of EPR effect [60–62]. MPA coated InAs/InP/ZnSe QDs (QD800-MPA) with emission maximum at about 800 nm showed very small size in HD (<10 nm). As shown in Fig. (4A), ultrasmall QD800-MPA nanoparticles pass through the normal blood vessels, and then extravasate from the vessels when they reach the angiogenic tumor vessels because of the leaky tumor vasculatures, finally, they accumulate preferentially at the tumor sites through the EPR effect because tumors lack an effective lymphatic drainage system. Using 22B and LS174T tumors as the models, *in vivo* fluorescence imaging showed that QD800-MPA was highly accumulated in the tumor area after 4 h postinjection (p.i.) with good fluorescence contrast from surrounding tissues (Fig. 4B). For the passive targeting of QDs, the circulation half-life should be long enough for the accumulation of QDs in tumors, while too long periods of time in blood circulation may result in the enhancement of toxicity to body.

Sentinel lymph node (SLN) imaging is clinically important since these are the sites where metastatic cancer cells are often found. Frangioni and Bawendi first reported the SLN mapping with NIR QDs in living subjects [18, 19, 63]. After the intradermal injection of NIR CdTe/CdSe QDs (~850 nm emission) into live mice and pigs, these QDs rapidly migrated to local SLNs and imaged virtually background-free (Fig. 5), which allows image-

guided resection of a one centimeter deep lymph node in a pig. After that, they also developed these type-II NIR QDs as noninvasive optical probes to do intraoperative SLN mapping in various locations of the body in adult pigs [64]. SLN mapping using QDs overcomes the limitations of currently available methods and provides highly sensitive, real-time visual feedback for image-guided localization and resection, which may be useful for fluorescence-guided surgery and might eventually permit potential mapping of SLNs and lymphatic flow in patients.

4.2. Peptide Conjugated QDs

Peptides are short polymers formed from the linkage of α -amino acids in a designed order. Because blood vessels express molecular markers that distinguish the vasculature of individual organs, tissues, and tumors, it is a general strategy to search for peptides that recognize tumor-specific vessels other than blood vessels by combining *ex vivo* and *in vivo* phase display. Ruoslahti *et al.* first reported selective targeting of peptides conjugated QDs *in vitro* and *in vivo* [65]. They described three kinds of peptides: CGFECVRQCPERC (denoted as GFE) which binds to membrane dipeptidase on the endothelial cells, KDEPQRRSARLSAKPAPPKPEPKP KKAPAKK (denoted as F3) which preferentially binds to blood vessels and tumor cells in various tumors, and CGNKRTRGC (denoted as LyP-1) which recognizes lymphatic vessels and tumor cells in certain tumors [66, 67]. These pioneering reports demonstrated the feasibility of specific targeting of QDs *in vivo* and opened up a new avenue to the biomedical applications of QDs, although the visible QDs is not optimal for *in vivo* imaging.

Recently, Chen *et al.* reported *in vivo* targeted imaging of tumor vasculature using peptide-conjugated NIR QDs [46, 47]. Cell adhesion molecule integrin $\alpha_v\beta_3$ is highly expressed on activated endothelial cells and tumor cells but is not readily detectable in resting endothelial cells and most normal organ systems. Integrin $\alpha_v\beta_3$ is a key player in tumor angiogenesis, progression, and spread. Moreover, integrin $\alpha_v\beta_3$ is expressed on both tumor vasculature and tumor cells. The arginine-glycine-aspartic acid (RGD)-containing components specifically bind to integrin $\alpha_v\beta_3$ in interstitial matrix [68]. After the conjugation of QD705 from Invitrogen (emission maximum at 705 nm) with RGD peptide, QD705-RGD exhibited high affinity of integrin $\alpha_v\beta_3$ in cell culture and *in vivo*, as shown in Fig. (6). After the tail vein injection of QD705-RGD into mice bearing subcutaneous integrin $\alpha_v\beta_3$ -positive U87MG human glioblastoma tumors, *in vivo* NIR fluorescence imaging indicated tumor intensity reached a maximum at 6 h p.i. with good contrast (tumor-to-background ratio was 4.42 ± 1.88).

Furthermore, Chen *et al.* chose non-cadmium NIR QDs (InAs/InP/ZnSe core/shell/shell nanoparticles with *emission maximum at about 800 nm*) as the low-toxic and efficient fluorescence probe to demonstrate the high specific targeting in the integrin $\alpha_v\beta_3$ -positive tumor vasculature after the surface modification of the RGD peptide [69]. After the PEG coating with the amine terminal functional group, it is facile to conjugate QD800-PEG with thiolated peptides (e.g., RGD and RAD). As shown in Fig. (7), the fluorescence imaging (IVIS Imaging System) indicated the tumor uptake of QD800-RGD was much higher than those of QD800-PEG and QD800-RAD. The semi-quantitative analysis of region of interest (ROI) showed high tumor uptake of 10.7 ± 1.5 %ID/g in the mice injected with QD800-RGD, while the tumor uptakes of QD800-PEG and QD800-RAD were 2.9 ± 0.3 %ID/g and 4.0 ± 0.5 %ID/g, respectively, indicating the specific tumor targeting of QD800-RGD.

The size of these QD-RGD (~20 nm in HD) prevented efficient extravasation, thus QD-RGD mainly targeted tumor vasculature instead of tumor cells. Immunofluorescence staining of the tumor vessels indicated that the majority of the QD fluorescence signal in the tumor colocalized with the tumor vessels, which was further confirmed by intravital imaging

of QD800-RGD in real-time [70]. As shown in Fig. (8), QD800-RGD did not extravasate in an SKOV-3 mouse ear tumor model, and they specifically bind their target in tumor neovasculature as aggregates, but no binding happened in control conditions. The high reproducibility of bioconjugation between QDs and RGD peptide and the feasibility of QD-RGD bioconjugates as tumor-targeted fluorescence probes warrant the successful applications of QDs for *in vivo* molecular imaging and diagnosis, which may aid in cancer detection and management including image-guided surgery.

4.3. Antibody Conjugated QDs

Antibodies are gamma globulin proteins that are found in blood or other bodily fluids of vertebrates, and they can identify and neutralize foreign objects (e.g., bacteria and viruses) by the immune system. The most common application of antibodies is to identify and locate intracellular and extracellular proteins that different cell types express. In 2004, Nie *et al.* first reported the prostate cancer targeting and fluorescence imaging *in vivo* using QDs conjugated prostate specific membrane antigen (PSMA)-specific monoclonal antibodies [57]. The fluorescence imaging indicated the high tumor targeting after the injection of QD-PSMA Ab conjugates, although the imaging contrast was moderate in visible window because of low tissue penetration and high autofluorescence. Using NIR QDs as fluorescence probes, Chung *et al.* demonstrated the highly sensitive detection of human C4-2 and C4-2B prostate tumors in mice after the surface functionalization of the anti-PSMA antibody [71].

Recently, Tada *et al.* reported the tracking of a single particle QD conjugated with the tumor-targeting antibody in tumors of living mice using a dorsal skinfold chamber and a high-speed confocal microscope with a high-sensitivity camera [72]. After the conjugation of QDs and monoclonal anti-HER2 antibody, they injected the QD-antibody into mice with HER2-overexpressing breast cancer to analyze the molecular processes of its mechanistic delivery to the tumor. They claimed there were six processes of delivery: initially in the circulation within a blood vessel, during extravasation, in the extracellular region, binding to HER2 on the cell membrane, moving from the cell membrane to the perinuclear region, and in the perinuclear region. The movement of the QD-antibody at each stage was “stop-and-go”. Although it is still unclear whether the “stop and go” pattern is typical for majority of injected QD conjugates or just a small subset of QDs, the image analysis of the delivery processes of single QD *in vivo* will be extremely important on molecular imaging and become a cutting-edge research field. Meanwhile, the research on the conjugation of QDs and antibody is attracting more and more attentions in the application of molecular imaging [9, 48, 49, 73, 74].

5. MULTIMODALITY IMAGING BASED ON NIR QUANTUM DOTS

Combination of multiple modalities can yield complementary information and offer synergistic advantages over any modality alone. Nanoparticles have the advantages in multifunctionality and enormous flexibility, which allow for the integration of therapeutic components, targeting ligands, and multimodality imaging probes into one entity. Quantitative and synergistic imaging of tumor angiogenesis will lead to more robust, reliable, and effective monitoring of personalized molecular cancer therapy. The future of tumor angiogenesis imaging lies in multimodality, and nanoflat-form-based imaging will be one of most important approach in multimodality imaging. Based on the QDs as optical probes, one can integrate MRI contrast agents [75–79], radio-nuclides [44, 80], or therapeutic drugs that combining diagnostics and therapy [81].

Recently, Chen *et al.* described the quantitative tumor targeting efficacy of dual-functional QD-based probes using both PET and NIR fluorescence imaging [44, 45]. Dual-modality

PET/NIR fluorescence imaging probes offer synergistic advantages over the single modality imaging probes by overcoming the low quantitative analysis of fluorescence intensity *in vivo* and *ex vivo*. Non-invasive PET imaging using radiolabeled QD conjugates can provide a robust and reliable measure of the *in vivo* biodistribution of QDs [80]. As shown in Fig. (9), they conjugated NIR QDs with VEGF protein and DOTA chelator for VEGFR-targeted PET/NIR fluorescence imaging after ^{64}Cu -labeling and evaluated the targeting efficacy *in vitro* and *in vivo* through cell-binding assay, cell staining, *in vivo* optical/PET imaging, *ex vivo* optical/PET imaging, and immunostaining histology analysis [45]. Although the stability and physicochemical properties of QDs after the radionuclides labeling should be concerned, with the further improvement in QD technology, it is expected that the accurate evaluation of *in vivo* tumor targeting efficacy using these dual-modality probes may significantly facilitate applications of QDs in biomedical science as well as clinical benefits.

6. CONCLUSION AND PERSPECTIVE

In this review, we have summarized the recent development of tumor imaging *in vivo* using NIR QDs as fluorescence probes. Nanotechnology indeed has the potential to significantly impact cancer diagnosis and cancer patient management. QDs have already fulfilled some of their promises as a new class of molecular probes for cancer research. However, there are still many considerable challenges and issues remained for the *in vivo* applications of NIR QDs. Besides the purity, dispersity, and stability of QDs in physiological environments, the variable physicochemical properties of each type of QDs may result in the unexpected behavior of QDs *in vivo*. The fundamental investigation of QD physicochemical properties is very important for the systematical analysis in the biodistribution of QDs. Several studies have shown QDs may be systemically distributed in organs and tissues. The absorption, distribution, metabolism, and excretion characteristics are highly variable for QDs because of the wide variation in QD physicochemical properties [82–84]. Moreover, QDs usually suffer from higher RES uptake and poorer extravasation comparing with small molecules or proteins. The majority research of QD is so far limited to vasculature-related disease, although the QDs with smaller size (normally <10 nm in HD) may extravasate from tumor angiogenic vessels because of EPR effect. Until now, it is still far away from QD-based imaging in small animals to scale up to *in vivo* imaging in patients due to the limited optical signal penetration depth. In clinical settings, optical imaging is relevant for tissues close to the surface of skin, tissues accessible by endoscopy, and intraoperative visualization. The major roadblocks for clinical translation of QDs are inefficient delivery, potential toxicity, and lack of quantification.

According to the potential toxicity *in vivo*, QD-based *ex vivo* protein nanosensors (e.g., FRET and BRET) [85–89] may be better choices for the future applications of QDs in cancer management. As shown in Fig. (10), patients can have their tumors biopsied and blood samples drawn for protein profiling by *ex vivo* nanosensors to detect and predict the response before and after the treatment without any potential side effects. *Ex vivo* diagnostics combining with *in vivo* imaging can markedly impact future cancer patient management by providing the synergistic information that neither strategy can provide alone. After further efforts, development, and validation, the major issues for clinical translation of QDs will become clearer and clearer, QD-based approaches (e.g., *ex vivo* nanosensor, *in vivo* imaging, and multimodality imaging) will eventually have the ability to predict and detect cancer in patients and monitor their response to personalized therapy.

Acknowledgments

This work was partially supported by NCI/NIH R21 CA121842 and U54 CA119367.

References

1. Roco MC. Nanotechnology: convergence with modern biology and medicine. *Curr Opin Biotechnol.* 2003; 14:337–346. [PubMed: 12849790]
2. Whitesides GM. The ‘right’ size in nanobiotechnology. *Nat Biotechnol.* 2003; 21:1161–1165. [PubMed: 14520400]
3. Bruchez M, Moronne M, Gin P, Weiss S, Alivisatos AP. Semiconductor nanocrystals as fluorescent biological labels. *Science.* 1998; 281:2013–2016. [PubMed: 9748157]
4. Resch-Genger U, Grabolle M, Cavaliere-Jaricot S, Nitschke R, Nann T. Quantum dots versus organic dyes as fluorescent labels. *Nat Methods.* 2008; 5:763–775. [PubMed: 18756197]
5. Mankoff DA. A definition of molecular imaging. *J Nucl Med.* 2007; 48:18N–21N.
6. Weissleder R. Molecular imaging in cancer. *Science.* 2006; 312:1168–1171. [PubMed: 16728630]
7. Weissleder R, Pittet MJ. Imaging in the era of molecular oncology. *Nature.* 2008; 452:580–589. [PubMed: 18385732]
8. Lim YT, Kim S, Nakayama A, Stott NE, Bawendi MG, Frangioni JV. Selection of quantum dot wavelengths for biomedical assays and imaging. *Mol Imaging.* 2003; 2:50–64. [PubMed: 12926237]
9. Jayagopal A, Russ PK, Haselton FR. Surface engineering of quantum dots for *in vivo* vascular imaging. *Bioconjug Chem.* 2007; 18:1424–1433. [PubMed: 17760416]
10. Diagaradjane P, Orenstein-Cardona JM, Colon-Casasnovas NE, Deorukhkar A, Shentu S, Kuno N, Schwartz DL, Gelovani JG, Krishnan S. Imaging epidermal growth factor receptor expression *in vivo*: Pharmacokinetic and biodistribution characterization of a bioconjugated quantum dot nanoprobe. *Clin Cancer Res.* 2008; 14:731–741. [PubMed: 18245533]
11. Lei Y, Tang H, Yao L, Yu R, Feng M, Zou B. Applications of mesenchymal stem cells labeled with Tat peptide conjugated quantum dots to cell tracking in mouse body. *Bioconjug Chem.* 2008; 19:421–427. [PubMed: 18081241]
12. Gao XL, Chen J, Chen JY, Wu BX, Chen HZ, Jiang XG. Quantum dots bearing lectin-functionalized nanoparticles as a platform for *in vivo* brain imaging. *Bioconjug Chem.* 2008; 19:2189–2195. [PubMed: 18922029]
13. Kikkeri R, Lepenies B, Adibekian A, Laurino P, Seeberger PH. *In vitro* imaging and *in vivo* liver targeting with carbohydrate capped quantum dots. *J Am Chem Soc.* 2009; 131:2110–2112. [PubMed: 19199612]
14. Smith AM, Duan HW, Mohs AM, Nie SM. Bioconjugated quantum dots for *in vivo* molecular and cellular imaging. *Adv Drug Deliv Rev.* 2008; 60:1226–1240. [PubMed: 18495291]
15. Cai WB, Chen XY. Nanoplatforms for targeted molecular imaging in living subjects. *Small.* 2007; 3:1840–1854. [PubMed: 17943716]
16. Yong KT, Roy I, Ding H, Bergey EJ, Prasad PN. Biocompatible near-infrared quantum dots as ultrasensitive probes for long-term *in vivo* imaging applications. *Small.* 2009; 5:1997–2004. [PubMed: 19466710]
17. Tsay JM, Pflughoeft M, Bentolila LA, Weiss S. Hybrid approach to the synthesis of highly luminescent CdTe/ZnS and CdHgTe/ZnS nanocrystals. *J Am Chem Soc.* 2004; 126:1926–1927. [PubMed: 14971912]
18. Kim S, Lim YT, Soltesz EG, De Grand AM, Lee J, Nakayama A, Parker JA, Mihaljevic T, Laurence RG, Dor DM, Cohn LH, Bawendi MG, Frangioni JV. Near-infrared fluorescent type II quantum dots for sentinel lymph node mapping. *Nat Biotechnol.* 2004; 22:93–97. [PubMed: 14661026]
19. Kim SW, Zimmer JP, Ohnishi S, Tracy JB, Frangioni JV, Bawendi MG. Engineering InAs_xP_{1-x}/InP/ZnSe III–V alloyed core/shell quantum dots for the near-infrared. *J Am Chem Soc.* 2005; 127:10526–10532. [PubMed: 16045339]
20. Allen PM, Bawendi MG. Ternary I3III3VI quantum dots luminescent in the red to near-infrared. *J Am Chem Soc.* 2008; 130:9240–9241. [PubMed: 18582061]
21. Xie RG, Peng XG. Synthesis of Cu-doped InP nanocrystals (d-dots) with ZnSe diffusion barrier as efficient and color-tunable NIR emitters. *J Am Chem Soc.* 2009; 131:10645–10651. [PubMed: 19588970]

22. Derfus AM, Chan WCW, Bhatia SN. Probing the cytotoxicity of semiconductor quantum dots. *Nano Lett.* 2004; 4:11–18.
23. Kirchner C, Liedl T, Kudera S, Pellegrino T, Javier AM, Gaub HE, Stolzle S, Fertig N, Parak WJ. Cytotoxicity of colloidal CdSe and CdSe/ZnS nanoparticles. *Nano Lett.* 2005; 5:331–338. [PubMed: 15794621]
24. Xie RG, Rutherford M, Peng XG. Formation of High-Quality I-III-VI Semiconductor Nanocrystals by Tuning Relative Reactivity of Cationic Precursors. *J Am Chem Soc.* 2009; 131:5691–5697. [PubMed: 19331353]
25. Sun YP, Zhou B, Lin Y, Wang W, Fernando KAS, Pathak P, Meziani MJ, Harruff BA, Wang X, Wang HF, Luo PJG, Yang H, Kose ME, Chen BL, Veca LM, Xie SY. Quantum-sized carbon dots for bright and colorful photoluminescence. *J Am Chem Soc.* 2006; 128:7756–7757. [PubMed: 16771487]
26. Gill R, Zayats M, Willner I. Semiconductor quantum dots for bioanalysis. *Angew Chem, Int Ed.* 2008; 47:7602–7625.
27. Chan WCW, Nie SM. Quantum dot bioconjugates for ultrasensitive nonisotopic detection. *Science.* 1998; 281:2016–2018. [PubMed: 9748158]
28. Xie RG, Chen K, Chen XY, Peng XG. InAs/InP/ZnSe core/shell/shell quantum dots as near-infrared emitters: bright, narrow-band, non-cadmium containing, and biocompatible. *Nano Res.* 2008; 1:457–464. [PubMed: 20631914]
29. Gao JH, Chen K, Xie RG, Xie J, Lee S, Cheng Z, Peng XG, Chen XY. Ultrasmall near-infrared non-cadmium quantum dots for *in vivo* tumor imaging. *Small.* 2010; 6:256–261. [PubMed: 19911392]
30. Rogach AL, Franzl T, Klar TA, Feldmann J, Gaponik N, Lesnyak V, Shavel A, Eychmuller A, Rakovich YP, Donegan JF. Aqueous synthesis of thiol-capped CdTe nanocrystals: State-of-the-art. *J Phys Chem C.* 2007; 111:14628–14637.
31. Mattoussi H, Mauro JM, Goldman ER, Anderson GP, Sundar VC, Mikulec FV, Bawendi MG. Self-assembly of CdSe-ZnS quantum dot bioconjugates using an engineered recombinant protein. *J Am Chem Soc.* 2000; 122:12142–12150.
32. Clapp AR, Goldman ER, Mattoussi H. Capping of CdSe-ZnS quantum dots with DHLA and subsequent conjugation with proteins. *Nat Protoc.* 2006; 1:1258–66. [PubMed: 17406409]
33. Uyeda HT, Medintz IL, Jaiswal JK, Simon SM, Mattoussi H. Synthesis of compact multidentate ligands to prepare stable hydrophilic quantum dot fluorophores. *J Am Chem Soc.* 2005; 127:3870–3878. [PubMed: 15771523]
34. Susumu K, Uyeda HT, Medintz IL, Pons T, Delehanty JB, Mattoussi H. Enhancing the stability and biological functionalities of quantum dots *via* compact multifunctional ligands. *J Am Chem Soc.* 2007; 129:13987–13996. [PubMed: 17956097]
35. Bauml M, Stamou D, Segura JM, Hovius R, Vogel H. Highly fluorescent streptavidin-coated CdSe nanoparticles: Preparation in water, characterization, and micropatterning. *Langmuir.* 2004; 20:3828–3831. [PubMed: 15969364]
36. Pinaud F, King D, Moore HP, Weiss S. Bioactivation and cell targeting of semiconductor CdSe/ZnS nanocrystals with phytochelatin-related peptides. *J Am Chem Soc.* 2004; 126:6115–6123. [PubMed: 15137777]
37. Liu YC, Brandon R, Cate M, Peng XG, Stony R, Johnson M. Detection of pathogens using luminescent CdSe/ZnS dendron nanocrystals and a porous membrane immunofilter. *Anal Chem.* 2007; 79:8796–8802. [PubMed: 17939743]
38. Dubertret B, Skourides P, Norris DJ, Noireaux V, Brivanlou AH, Libchaber A. *In vivo* imaging of quantum dots encapsulated in phospholipid micelles. *Science.* 2002; 298:1759–1762. [PubMed: 12459582]
39. Ballou B, Lagerholm BC, Ernst LA, Bruchez MP, Waggoner AS. Noninvasive imaging of quantum dots in mice. *Bioconjug Chem.* 2004; 15:79–86. [PubMed: 14733586]
40. Carion O, Mahler B, Pons T, Dubertret B. Synthesis, encapsulation, purification and coupling of single quantum dots in phospholipid micelles for their use in cellular and *in vivo* imaging. *Nat Protoc.* 2007; 2:2383–2390. [PubMed: 17947980]

41. Yu WW, Chang E, Falkner JC, Zhang JY, Al-Somali AM, Sayes CM, Johns J, Drezek R, Colvin VL. Forming biocompatible and nonaggregated nanocrystals in water using amphiphilic polymers. *J Am Chem Soc.* 2007; 129:2871–2879. [PubMed: 17309256]
42. Liu W, Howarth M, Greytak AB, Zheng Y, Nocera DG, Ting AY, Bawendi MG. Compact biocompatible quantum dots functionalized for cellular imaging. *J Am Chem Soc.* 2008; 130:1274–1284. [PubMed: 18177042]
43. Michalet X, Pinaud FF, Bentolila LA, Tsay JM, Doose S, Li JJ, Sundaresan G, Wu AM, Gambhir SS, Weiss S. Quantum dots for live cells, *in vivo* imaging, and diagnostics. *Science.* 2005; 307:538–544. [PubMed: 15681376]
44. Cai WB, Chen K, Li ZB, Gambhir SS, Chen XY. Dual-function probe for PET and near-infrared fluorescence imaging of tumor vasculature. *J Nucl Med.* 2007; 48:1862–1870. [PubMed: 17942800]
45. Chen K, Li ZB, Wang H, Cai WB, Chen XY. Dual-modality optical and positron emission tomography imaging of vascular endothelial growth factor receptor on tumor vasculature using quantum dots. *Eur J Nucl Med Mol Imaging.* 2008; 35:2235–2244. [PubMed: 18566815]
46. Cai WB, Shin DW, Chen K, Gheysens O, Cao QZ, Wang SX, Gambhir SS, Chen XY. Peptide-labeled near-infrared quantum dots for imaging tumor vasculature in living subjects. *Nano Lett.* 2006; 6:669–676. [PubMed: 16608262]
47. Cai WB, Chen XY. Preparation of peptide-conjugated quantum dots for tumor vasculature-targeted imaging. *Nat Protoc.* 2008; 3:89–96. [PubMed: 18193025]
48. Pathak S, Davidson MC, Silva GA. Characterization of the functional binding properties of antibody conjugated quantum dots. *Nano Lett.* 2007; 7:1839–1845. [PubMed: 17536868]
49. Lao UL, Mulchandani A, Chen W. Simple conjugation and purification of quantum dot-antibody complexes using a thermally responsive elastin-protein L scaffold as immunofluorescent agents. *J Am Chem Soc.* 2006; 128:14756–14757. [PubMed: 17105256]
50. Medintz IL, Clapp AR, Brunel FM, Tiefenbrunn T, Uyeda HT, Chang EL, Deschamps JR, Dawson PE, Mattoussi H. Proteolytic activity monitored by fluorescence resonance energy transfer through quantum-dot-peptide conjugates. *Nat Mater.* 2006; 5:581–589. [PubMed: 16799548]
51. Medintz IL, Berti L, Pons T, Grimes AF, English DS, Alessandrini A, Facci P, Mattoussi H. A reactive peptidic linker for self-assembling hybrid quantum dot-DNA bioconjugates. *Nano Lett.* 2007; 7:1741–1748. [PubMed: 17530814]
52. Lin PC. Optical imaging and tumor angiogenesis. *J Cell Biochem.* 2003; 90:484–491. [PubMed: 14523982]
53. Cai WB, Hsu AR, Li ZB, Chen XY. Are quantum dots ready for *in vivo* imaging in human subjects? *Nanoscale Res Lett.* 2007; 2:265–281. [PubMed: 21394238]
54. Ntziachristos V, Bremer C, Weissleder R. Fluorescence imaging with near-infrared light: new technological advances that enable *in vivo* molecular imaging. *Eur Radiol.* 2003; 13:195–208. [PubMed: 12541130]
55. Frangioni JV. *In vivo* near-infrared fluorescence imaging. *Curr Opin Chem Biol.* 2003; 7:626–634. [PubMed: 14580568]
56. Carmeliet P, Jain RK. Angiogenesis in cancer and other diseases. *Nature.* 2000; 407:249–257. [PubMed: 11001068]
57. Gao XH, Cui YY, Levenson RM, Chung LWK, Nie SM. *In vivo* cancer targeting and imaging with semiconductor quantum dots. *Nat Biotechnol.* 2004; 22:969–976. [PubMed: 15258594]
58. Kratz F, Muller IA, Ryppa C, Warnecke A. Prodrug strategies in anticancer chemotherapy. *ChemMedChem.* 2008; 3:20–53. [PubMed: 17963208]
59. Choi HS, Liu WH, Misra P, Tanaka E, Zimmer JP, Ipe BI, Bawendi MG, Frangioni JV. Renal clearance of quantum dots. *Nat Biotechnol.* 2007; 25:1165–1170. [PubMed: 17891134]
60. Park JH, Gu L, von Maltzahn G, Ruoslahti E, Bhatia SN, Sailor MJ. Biodegradable luminescent porous silicon nanoparticles for *in vivo* applications. *Nat Mater.* 2009; 8:331–336. [PubMed: 19234444]
61. Maeda H. The enhanced permeability and retention (EPR) effect in tumor vasculature: The key role of tumor-selective macromolecular drug targeting. *Adv Enzyme Regul.* 2001; 41:189–207. [PubMed: 11384745]

62. Cho KJ, Wang X, Nie SM, Chen Z, Shin DM. Therapeutic nanoparticles for drug delivery in cancer. *Clin Cancer Res.* 2008; 14:1310–1316. [PubMed: 18316549]
63. Zimmer JP, Kim SW, Ohnishi S, Tanaka E, Frangioni JV, Bawendi MG. Size series of small indium arsenide-zinc selenide core-shell nanocrystals and their application to *in vivo* imaging. *J Am Chem Soc.* 2006; 128:2526–2527. [PubMed: 16492023]
64. Soltesz EG, Kim S, Laurence RG, DeGrand AM, Parungo CP, Dor DM, Cohn LH, Bawendi MG, Frangioni JV, Mihaljevic T. Intraoperative sentinel lymph node mapping of the lung using near-infrared fluorescent quantum dots. *Ann Thorac Surg.* 2005; 79:269–277. [PubMed: 15620956]
65. Akerman ME, Chan WCW, Laakkonen P, Bhatia SN, Ruoslahti E. Nanocrystal targeting *in vivo*. *Proc Natl Acad Sci USA.* 2002; 99:12617–12621. [PubMed: 12235356]
66. Porkka K, Laakkonen P, Hoffman JA, Bernasconi M, Ruoslahti E. A fragment of the HMGN2 protein homes to the nuclei of tumor cells and tumor endothelial cells *in vivo*. *Proc Natl Acad Sci USA.* 2002; 99:7444–7449. [PubMed: 12032302]
67. Laakkonen P, Porkka K, Hoffman JA, Ruoslahti E. A tumor-homing peptide with a targeting specificity related to lymphatic vessels. *Nat Med.* 2002; 8:751–755. [PubMed: 12053175]
68. Xiong JP, Stehle T, Zhang RG, Joachimiak A, Frech M, Goodman SL, Aranout MA. Crystal structure of the extracellular segment of integrin alpha V beta 3 in complex with an Arg-Gly-Asp ligand. *Science.* 2002; 296:151–155. [PubMed: 11884718]
69. Gao JH, Chen K, Xie RG, Xie J, Yan YJ, Cheng Z, Peng XG, Chen XY. *In vivo* tumor-targeted fluorescence imaging using near-infrared non-cadmium quantum dots. *Bioconjug Chem.* 2010; 21(4):604–609. [PubMed: 20369817]
70. Smith BR, Cheng Z, De A, Koh AL, Sinclair R, Gambhir SS. Real-time intravital imaging of RGD-quantum dot binding to luminal endothelium in mouse tumor neovasculature. *Nano Lett.* 2008; 8:2599–2606. [PubMed: 18386933]
71. Shi CM, Zhu Y, Xie ZH, Qian WP, Hsieh CL, Nie SM, Su YP, Zhau HE, Chung LWK. Visualizing human prostate cancer cells in mouse skeleton using bioconjugated near-infrared fluorescent quantum dots. *Urology.* 2009; 74:446–451. [PubMed: 19428067]
72. Tada H, Higuchi H, Wanatabe TM, Ohuchi N. *In vivo* real-time tracking of single quantum dots conjugated with monoclonal anti-HER2 antibody in tumors of mice. *Cancer Res.* 2007; 67:1138–1144. [PubMed: 17283148]
73. Sun JT, Zhu MQ, Fu K, Lewinski N, Drezek RA. Lead sulfide near-infrared quantum dot bioconjugates for targeted molecular imaging. *Int J Nanomed.* 2007; 2:235–240.
74. Bertolini G, Paleari L, Catassi A, Roz L, Cesario A, Sozzi G, Russo P. *In vivo* cancer imaging with semiconductor quantum dots. *Curr Pharm Anal.* 2008; 4:197–205.
75. Park JH, von Maltzahn G, Ruoslahti E, Bhatia SN, Sailor MJ. Micellar hybrid nanoparticles for simultaneous magneto-fluorescent imaging and drug delivery. *Angew Chem, Int Ed.* 2008; 47:7284–7288.
76. Ostendorp M, Douma K, Hackeng TM, Dirksen A, Post MJ, van Zandvoort MAM, Backes WH. Quantitative molecular magnetic resonance imaging of tumor angiogenesis using cNGR-labeled paramagnetic quantum dots. *Cancer Res.* 2008; 68:7676–7683. [PubMed: 18794157]
77. Gao JH, Zhang B, Gao Y, Pan Y, Zhang XX, Xu B. Fluorescent magnetic nanocrystals by sequential addition of reagents in a one-pot reaction: a simple preparation for multifunctional nanostructures. *J Am Chem Soc.* 2007; 129:11928–11935. [PubMed: 17824703]
78. Gao JH, Zhang W, Huang PB, Zhang B, Zhang XX, Xu B. Intracellular spatial control of fluorescent magnetic nanoparticles. *J Am Chem Soc.* 2008; 130:3710–3711. [PubMed: 18314984]
79. Gao JH, Gu HW, Xu B. Multifunctional magnetic nanoparticles: design, synthesis, and biomedical applications. *Acc Chem Res.* 2009; 42:1097–1107. [PubMed: 19476332]
80. Schipper ML, Iyer G, Koh AL, Cheng Z, Ebenstein Y, Aharoni A, Keren S, Bentolila LA, Li JQ, Rao JH, Chen XY, Banin U, Wu AM, Sinclair R, Weiss S, Gambhir SS. Particle size, surface coating, and PEGylation influence the biodistribution of quantum dots in living mice. *Small.* 2009; 5:126–134. [PubMed: 19051182]
81. Weng KC, Noble CO, Papahadjopoulos-Sternberg B, Chen FF, Drummond DC, Kirpotin DB, Wang DH, Hom YK, Hann B, Park JW. Targeted tumor cell internalization and imaging of

- multifunctional quantum dot-conjugated immunoliposomes *in vitro* and *in vivo*. Nano Lett. 2008; 8:2851–2857. [PubMed: 18712930]
82. Hoshino A, Fujioka K, Oku T, Suga M, Sasaki YF, Ohta T, Yasuhara M, Suzuki K, Yamamoto K. Physicochemical properties and cellular toxicity of nanocrystal quantum dots depend on their surface modification. Nano Lett. 2004; 4:2163–2169.
83. Hardman R. A toxicologic review of quantum dots: Toxicity depends on physicochemical and environmental factors. Environ Health Perspect. 2006; 114:165–172. [PubMed: 16451849]
84. Lewinski N, Colvin V, Drezek R. Cytotoxicity of nanoparticles. Small. 2008; 4:26–49. [PubMed: 18165959]
85. Medintz IL, Clapp AR, Mattoussi H, Goldman ER, Fisher B, Mauro JM. Self-assembled nanoscale biosensors based on quantum dot FRET donors. Nat Mater. 2003; 2:630–638. [PubMed: 12942071]
86. Zhang CY, Yeh HC, Kuroki MT, Wang TH. Single-quantum-dot-based DNA nanosensor. Nat Mater. 2005; 4:826–31. [PubMed: 16379073]
87. So MK, Xu CJ, Loening AM, Gambhir SS, Rao JH. Self-illuminating quantum dot conjugates for *in vivo* imaging. Nat Biotechnol. 2006; 24:339–343. [PubMed: 16501578]
88. Yao HQ, Zhang Y, Xiao F, Xia ZY, Rao JH. Quantum dot/bioluminescence resonance energy transfer based highly sensitive detection of proteases. Angew Chem Int Ed. 2007; 46:4346–4349.
89. Boeneman K, Mei BC, Dennis AM, Bao G, Deschamps JR, Mattoussi H, Medintz IL. Sensing caspase 3 activity with quantum dot-fluorescent protein assemblies. J Am Chem Soc. 2009; 131:3828–3829. [PubMed: 19243181]

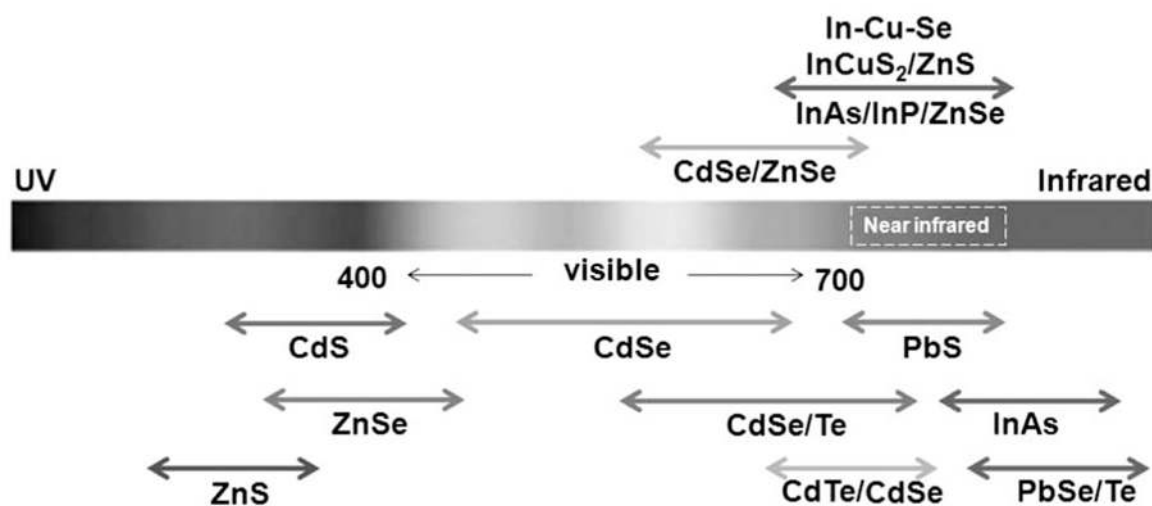


Fig. 1. Representative QDs with different materials scaled as a function of their emission wavelengths superimposed over the spectrum. There are several kinds of QDs with the emission wavelength in the NIR region.

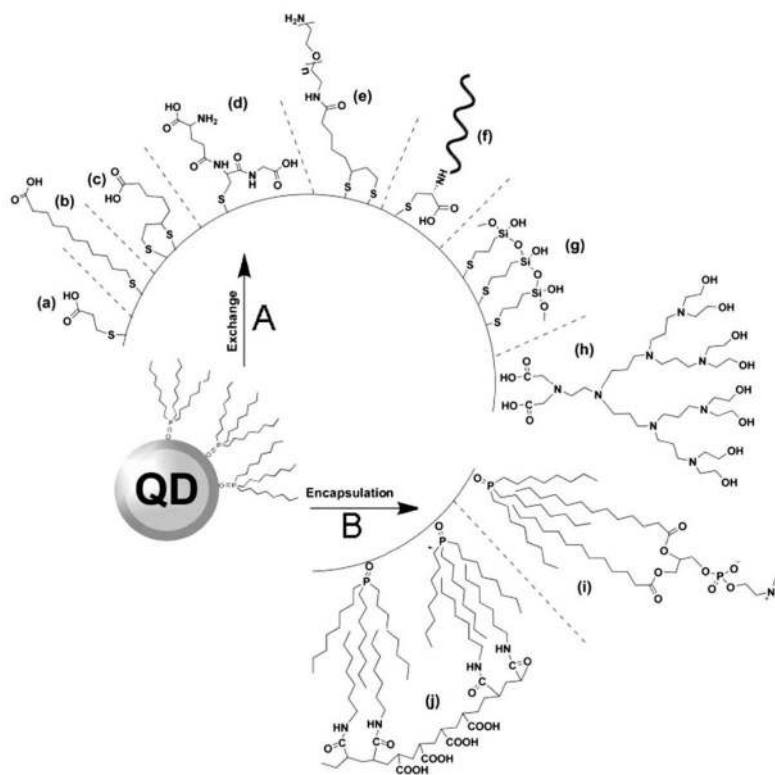
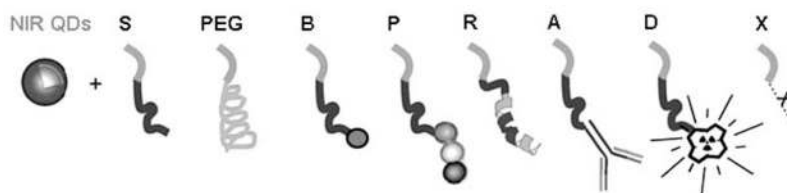


Fig. 2.

Overview of strategies to prepare water-dispersible QDs. **(A)** Exchange of the organic surfactant layer with a water-soluble layer: **(a) – (d)** thiolated or dithiolated functional monolayers, **(e)** glutathione (GSH) layer, **(f)** cysteine-terminated peptides, **(g)** thiolated siloxane, and **(h)** carboxylic acid-functionalized dendrone. **(B)** Encapsulation of QDs stabilized with an organic encapsulating layer in functional bilayer films composed of **(i)** a phospholipid encapsulating layer, and **(j)** a diblock copolymer layer. Reprinted with permission from ref. [26]. Copyright 2008, Wiley-VCH.

**Fig. 3.**

The Overview of bioconjugation and functionalization on NIR QDs. S, solubilization sequence; PEG, polyethylene glycol; B, biotin; P, peptides; R, protein sequence; A, antibody; D, DOTA; X, any unspecified peptide-encoded function. QDs can be targeted with B, P, R, A, or other chemical moieties. For simultaneous PET and fluorescence imaging, QDs can be rendered radioactive by D chelation of radionuclides; for simultaneous MRI and fluorescence imaging, QDs can be rendered radioactive by D chelation of nuclear spin labels. Reprinted with permission from ref. [43]. Copyright 2005, AAAS.

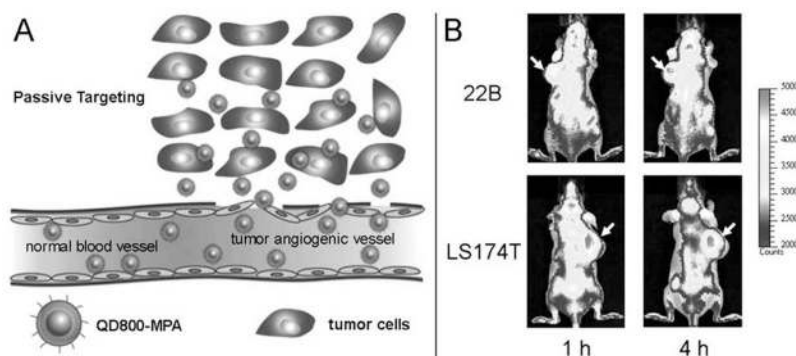


Fig. 4. Ultrasmall QD800-MPA for *in vivo* tumor imaging. (A) The structure of QD800-MPA and the illustration of the passive tumor targeting of QD800-MPA in tumor models. (B) *In vivo* NIR fluorescence imaging of 22B or LS174T (arrows) tumor-bearing mice at 1 h and 4 h after the tail vein injection of QD800-MPA. Reprinted with permission from ref. [29]. Copyright 2010, Wiley-VCH.

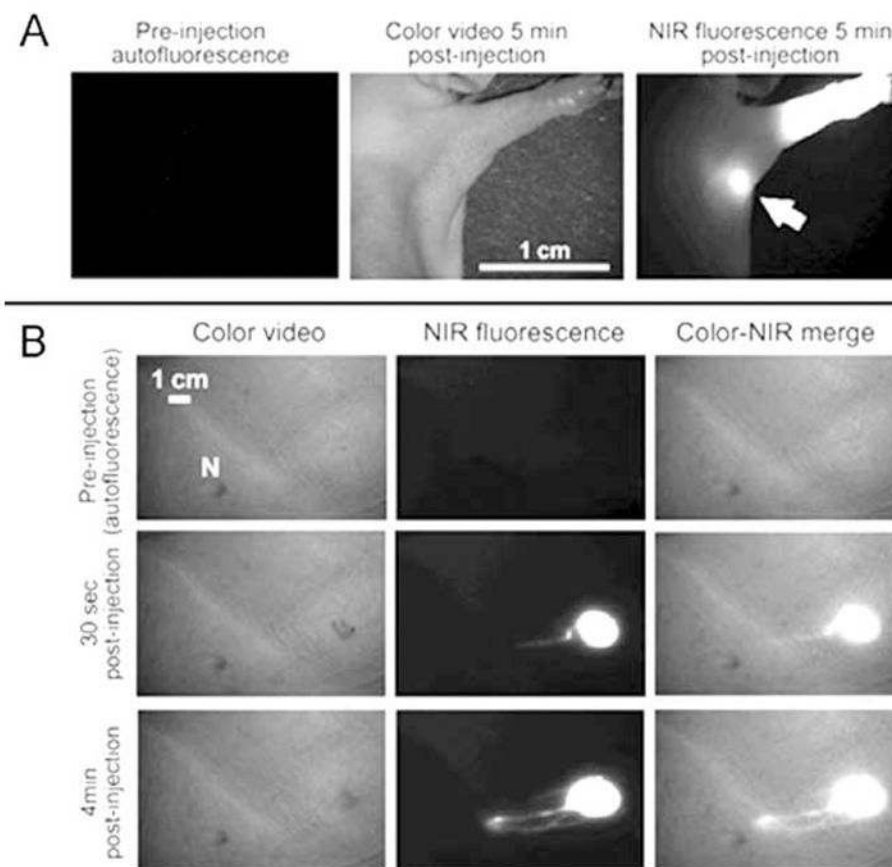


Fig. 5. Sentinel lymph node mapping in the mouse and pig using NIR QDs. **(A)** Images of mouse injected intradermally with 10 pmol of NIR QDs in the left paw. Left, pre-injection NIR autofluorescence image; middle, 5 min post-injection white light color video image; right, 5 min post-injection NIR fluorescence image. An arrow indicates the putative axillary sentinel lymph node. **(B)** Images of the surgical field in a pig injected intradermally with 400 pmol of NIR QDs in the right groin: before injection (autofluorescence), 30 s after injection, and 4 min after injection. The position of a nipple (N) is indicated. Reprinted with permission from ref. [18]. Copyright 2004, Nature Publishing Group.

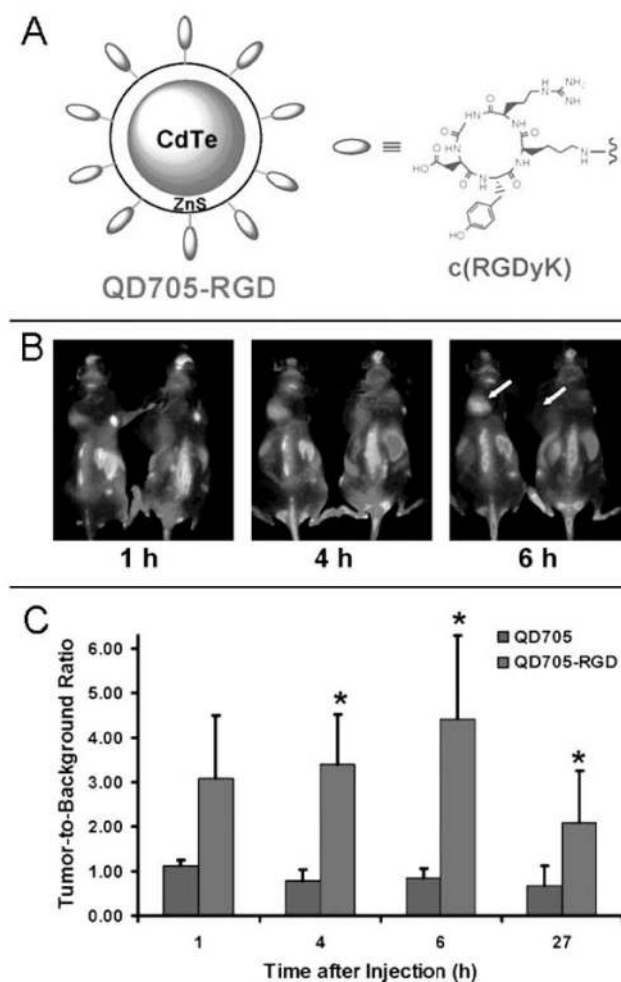


Fig. 6. RGD peptide-conjugated QD705 for NIR fluorescence imaging of tumor vasculature. **(A)** the schematic illustration of QD705-RGD. **(B)** *In vivo* fluorescence imaging of tumor vasculature in U87MG tumor-bearing mice at 1 h, 4 h, and 6 h after the tail vein injection of QD705-RGD (left) and QD705 (right). **(C)** Tumor-to-background ratios of mice injected with QD705 or QD705-RGD. Reprinted with permission from ref. [46]. Copyright 2006, American Chemical Society.

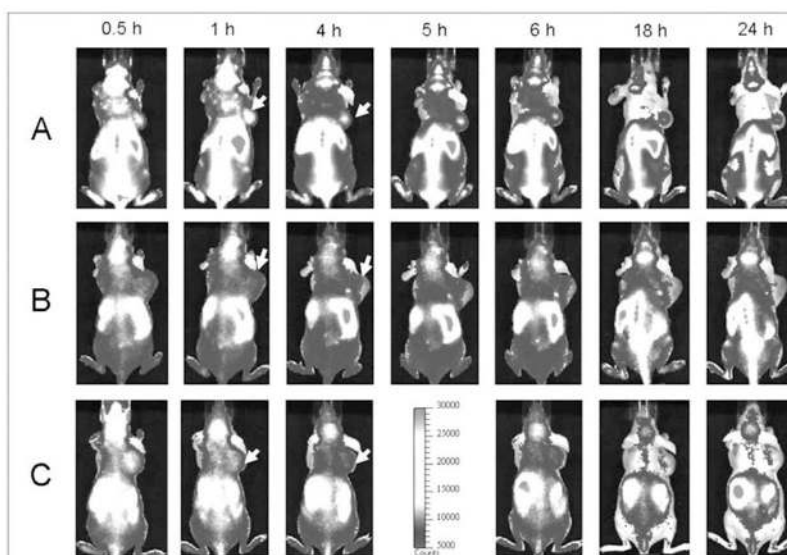
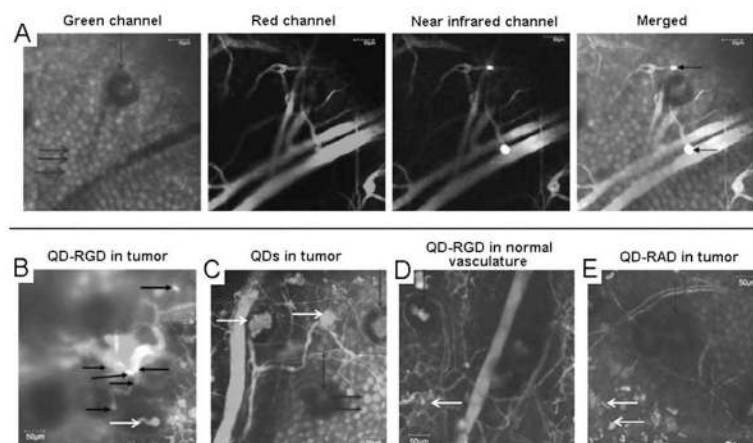


Fig. 7. Non-cadmium NIR QDs as the low-toxic and efficient fluorescence probe to image the integrin $\alpha_v\beta_3$ -positive tumor vasculature after the surface modification with the RGD peptide. *In vivo* fluorescence imaging of U87MG tumor-bearing mice (arrows) injected with (A) QD800-RGD, (B) QD800-PEG, and (C) QD800-RAD, respectively. Reprinted with permission from ref. [69]. Copyright 2010, American Chemical Society.

**Fig. 8.**

Direct visualization of binding of QD800-RGD to tumor vessel endothelium and controls.

(A) Panel displays different output channels of the identical imaging plane along the row. In the green channel, individual EGFP-expressing cancer cells are visible, while the red channel outlines the tumor's vasculature *via* injection of Angiosense dye. The NIR channel shows intravascularly administered QDs which remain in the vessels. Binding events are visible by reference to bright white signal. These are demarcated by arrows in the rightmost merged image, in which all three channels have been overlaid. (B) Merged image in a different mouse using QD800-RGD. Individual cells are not generally visible. (C–E) Typical images of no binding in each control condition: (C) Tumor neovasculature containing unconjugated QDs, (D) normal vasculature containing QD800-RGD, and (E) tumor neovasculature containing QD800-RAD. Reprinted with permission from ref. [70].

Copyright 2008, American Chemical Society.

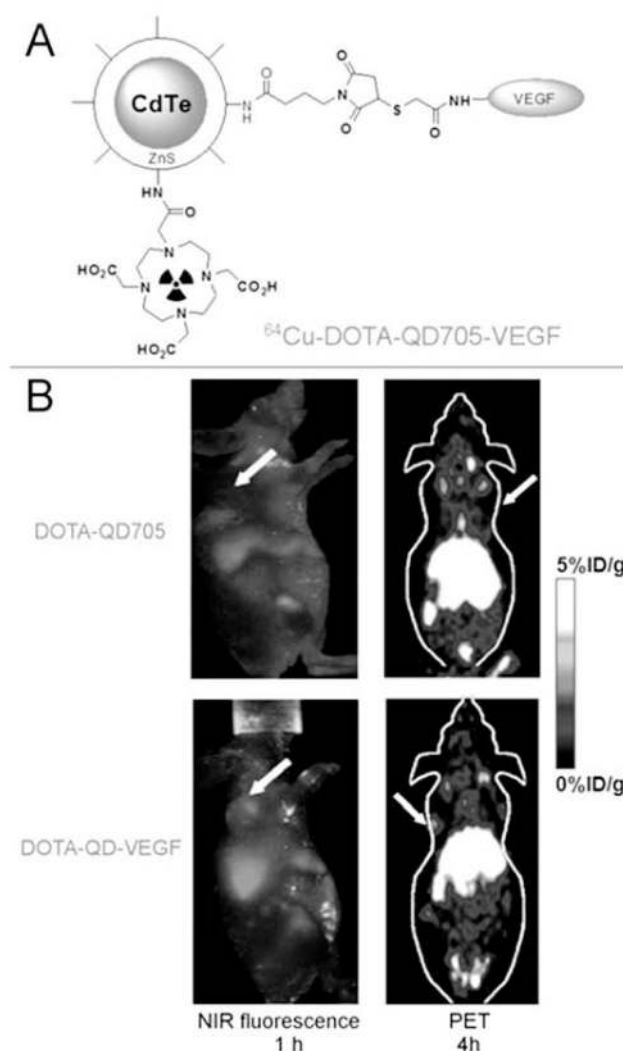


Fig. 9. Dual-modality optical and PET imaging of tumor VEGFR expression using radiolabeled NIR QDs. **(A)** The structure of ^{64}Cu -DOTA-QD705-VEGF conjugate. **(B)** *In vivo* fluorescence imaging and coronal PET imaging of U87MG tumor-bearing mice (arrows) at 1 h and 4 h after the tail vein injection of DOTA-QD705 and DOTA-QD705-VEGF, respectively.

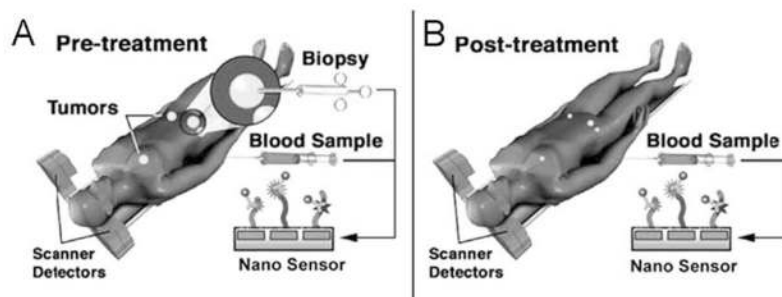


Fig. 10.

The *ex vivo* diagnostics of patients using NIR-emitting QDs as nanosensors. **(A)** Before treatment, patients can have their tumors biopsied and blood samples drawn for protein profiling by *ex vivo* nanosensors to predict their response to a given therapy. **(B)** During the treatment, patient response will be evaluated by blood analysis and molecular imaging to ensure the accurate differentiation of responders from non-responders.